Supporting Information

Efficient Synthesis of 2-Amino-4*H*-benzo[*b*]pyrans via Copper-periodic Mesoporous Organosilica Nanocomposites Catalyst in Aqueous Media

Roghaye Ramazannejad lori[1], Zahra Fahimeh alsadat Mortazavi[2*], Vajihe Nejadshafiee [3*], Asadollah Hassankhani[1]

[1] *Department of Chemistry, Graduate University of Advanced Technology, Kerman, Iran*

[2] *Department of Chemical Engineering, Sirjan University of Technology, Sirjan, Iran. Email: zahrafsmrtz@gmail.com*

[3] *Central Lab, Vali-e-Asr University, 77176, Rafsanjan, Iran. Email: v.nejadshafiee@vru.ac.ir*

1. Preparation of Cu@MOS NCs Catalyst **2**

2. Characterization of Cu@MOS NCs Catalyst **3**

3. FT-IR of the Synthesized Compounds **7**

4. ^{1}H NMR Spectra of Some Synthesized Compounds **12**

1- Preparation of Cu@MOS NCs Catalyst

Material and Physical Measurements

The cetyltrimethylammonium bromide (CTAB), tetraethylorthosilicate (TEOS), 3-chloropropyltrimethoxysilane, 1,3,5-triazine-2,4,6-triamine (melamine), salicylaldehyde and metal salts $Cu(CH_3COO)_2{\cdot}H_2O$, $Co(CH_3COO)_2{\cdot}6H_2O$, $Ni(NO_3)_2$ and $Zn(CH_3COO)_2{\cdot}2H_2O$ were supplied by Fluka, Aldrich and Merck Chemical Company. FT-IR spectra were obtained as KBr pellets on a Perkin-Elmer 781 spectrophotometer and on an impact 400 Nicolet FT-IR spectrophotometer. TGA was carried out on STA503 WinTA instrument at a heating rate of 10 ºC min^{-1} under nitrogen (N_2) atmosphere. The XRD patterns were recorded on an X-ray diffractometer (Bruker, D8 ADVANCE, Germany) using a Cu-Ka radiation (λ = 0.154056 nm) in the range 2θ = 0.5–5°. The N_2 adsorption/desorption analysis (BET) was performed at –196 °C using an automated gas adsorption analyzer (Tristar 3000, Micromeritics). The surface morphology of the supported catalyst was studied by scanning electron microscopy. FE-SEM and elemental analysis were carried out using a Jeol SEM instrument (model VEGA/TESCAN) combined with an INCA instrument for energy dispersive X-ray spectroscopy scanning electron microscopy (EDS-SEM), with scanning electron electrode at 15 kV. The DRS of samples was recorded at room temperature on Perkin-Elmer 35 LAMDA instrument using barium sulfate as a reference. ^{1}H NMR and ^{13}C NMR were recorded in $CDCl_3$ and DMSO-d_6 solvents on a Bruker DRX-400 spectrometer with tetramethylsilane as internal reference.

The copper heterogeneous catalyst was prepared by loading copper metal onto mesoporous organosilica nanocomposites (Cu@MOS NCs). The MSO structure was synthesized in sol-gel process and under hydrothermal condition via three steps: **1)** To preparation of copper complex: Melamine derivate (Ligand, 1 mmol) and copper acetate monohydrate (1 mmol) in dimethylformamide solvent (15 mL) under reflux for 3 h. The solid was filtered, washed with ethanol and dried for 12 h under vacuum oven. **2)** For synthesis of copper complex-organosilica: Copper complex (1.3 mmol) was dissolved in dry ethanol (60 mL), then 3-chloropropyltrimethoxysilane (2.6 mmol) and NaH (1 mmol) as a base was added to mixture and also, ascorbic acid (1 mmol) for the reduction of the Cu(II) to Cu(I) was added. The reaction mixture was stirred and heated for 14 h under N_2 atmosphere. The solid were washed with ether (2×30 mL) and dried under vacuum oven overnight at 40 °C.

3) To the preparation of Cu@MOS NCs: The CTAB as surfactant (2.74 mmol) was dissolved in distilled water (47 mL). Then ammonia (25 %, 11 mL) was added to mixture and stirred for 30 min to obtain a clear solution. The organometallic-silica copper complex (0.52 mmol) and TEOS (10 mmol) were added to the above solution and refluxed for 24 h. After in time, the solid was filtered and washed with DI water, and dried under vacuum oven for 10 h at 40 ºC. The CTAB compound was removed with HCl solution (0.05 M) at 50 ºC for 10 h (50 mL of 0.05 ethanolic HCl for 1 g of solid material).

2- Characterization of Cu@MOS NCs Catalyst

The N_2 adsorption–desorption isotherm and pore size distribution of Cu@MOS NCs hybrid mesoporous silica nanocomposite framework is shown in Figure S1. The isotherm exhibited type IV patterns with H3 hysteresis loops, which is a characteristics of mesoporous solids.[33] The BET specific surface area and a total pore volume were 462.40 $m^2 \cdot g^{-1}$ and 0.5 $cm^3 \cdot g^{-1}$, respectively (Figure S1a). The pore diameter is calculated according to the BJH model to be 3.98 nm (Figure S1b).

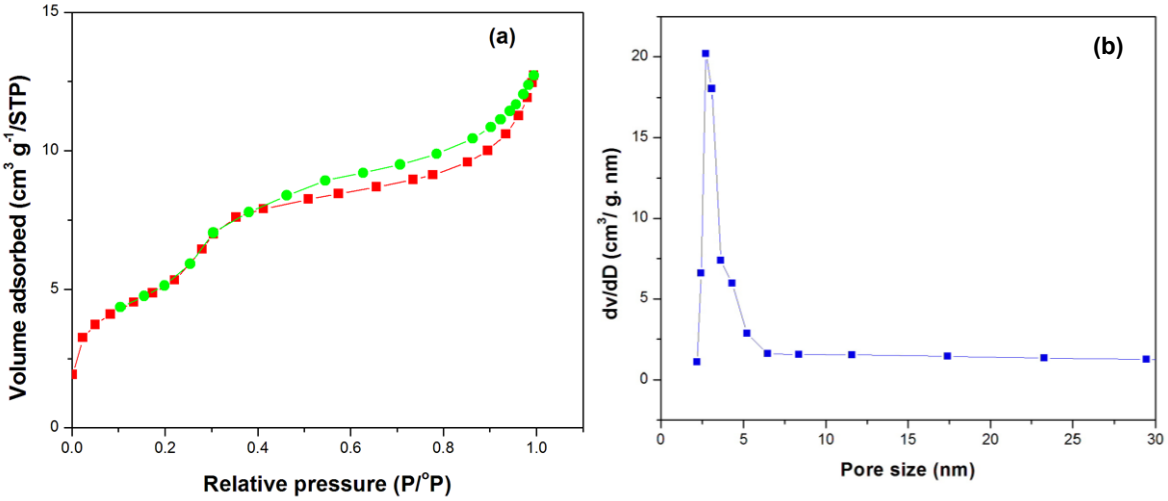

Figure S1. N_2 adsorption-desorption isotherm (a) and pore size distribution curve (b) of Cu@MOS NCs.

TGA of Cu@MOS NCs is shown in Figure S2. According to the thermogram, 3–4 % weight loss within a temperature range of around 100–300 ºC which is due to the loss of adsorbed water molecules. Furthermore, it shows that a degradation process occurs between 300–483 ºC and the weight loss is about 11–12%. This is due to the breakdown of copper imprinted periodic mesoporous organosilica nanocomposite groups imprinted to the MOS.

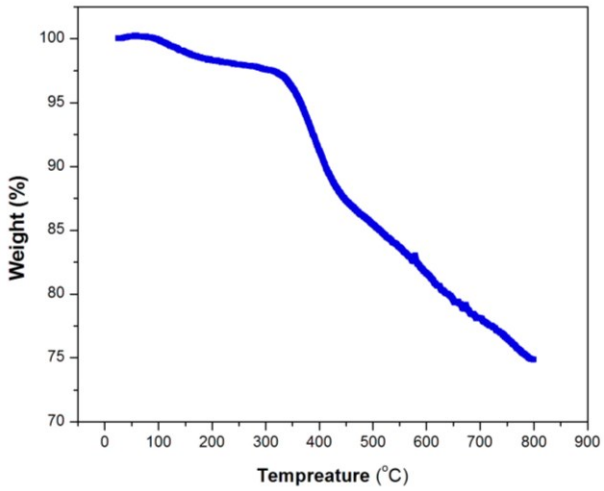

Figure S2. TGA thermograms of Cu@MOS NCs.

Figure S3a shows the SEM image of the Cu@MOS NCs which contain many short rods. Moreover, this surface morphology of the NPs catalyst is indicative the presence of a well ordered mesostructure with hexagonal lattice arrangements.

For Cu@MOS NCs, the obtained results by EDS were as followed: (%) C, 18.42; N, 7.09; Cu, 3.43; Si, 24.73; O, 49.34 (Figure S3b). The EDS analysis is confirmed the presence of Schiff base-copper complex (**2**) on PMO.

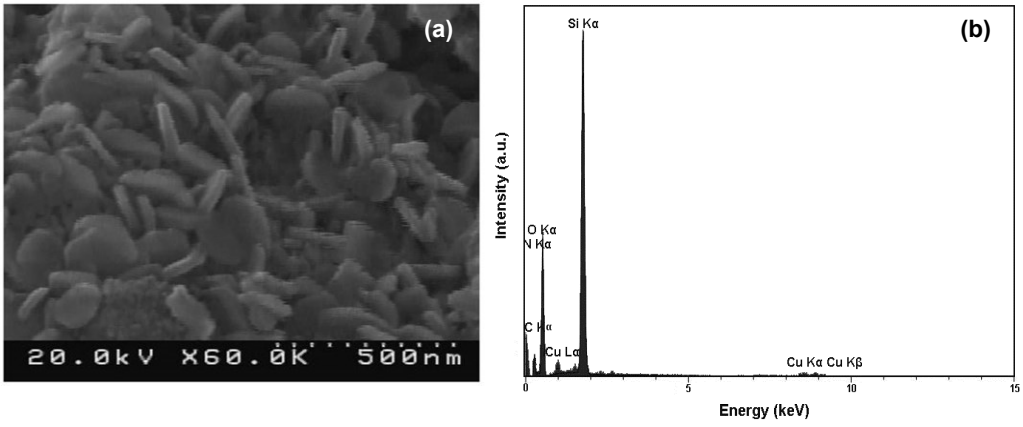

Figure S3. a) FE-SEM image of Cu@MOS NCs, b) EDS pattern of Cu@MOS NCs.

The well-ordered mesostructural arrangement of the Cu@MOS NCs hybrid was confirmed by low angle XRD. Figure S4 shows the low angle XRD patterns of Cu@MOS NCs. The three reflection peaks corresponding to 2θ = 0.5–5º of 1.05º, 1.9º and 2.3º were indexed to the (100), (110) and (200) reflections, respectively, which are clearly indicative of the presence of a well ordered mesostructure of the materials with hexagonal lattice arrangements.

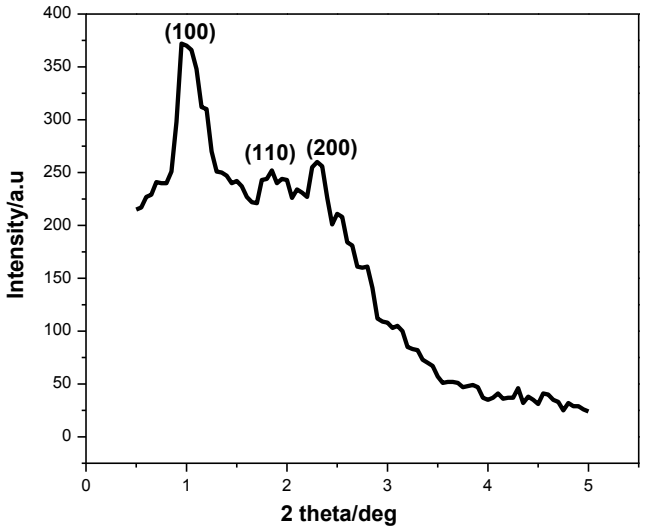

Figure S4. XRD spectrum of Cu@MOS NCs.

The FT-IR spectra of Cu@MOS NCs exhibited a broad band in the hydroxyl region 3367 cm^{-1}. The C=N stretching vibration frequency of Cu@MOS NCs was observed at 1561 cm^{-1}. The vibration bands at 2853 and 2923 cm^{-1} were assigned to the C–H stretching vibrations of propyl and methyl groups, respectively. The vibration peak at 1474 cm^{-1} was characteristic of N–C vibrations of the aromatic functional groups related to the Cu@MOS NCs. The band in the range 1000–1100 cm^{-1} was assigned to Si–O–Si groups and the band at 961 cm^{-1} was attributed to Si–OH groups (Figure S5c).

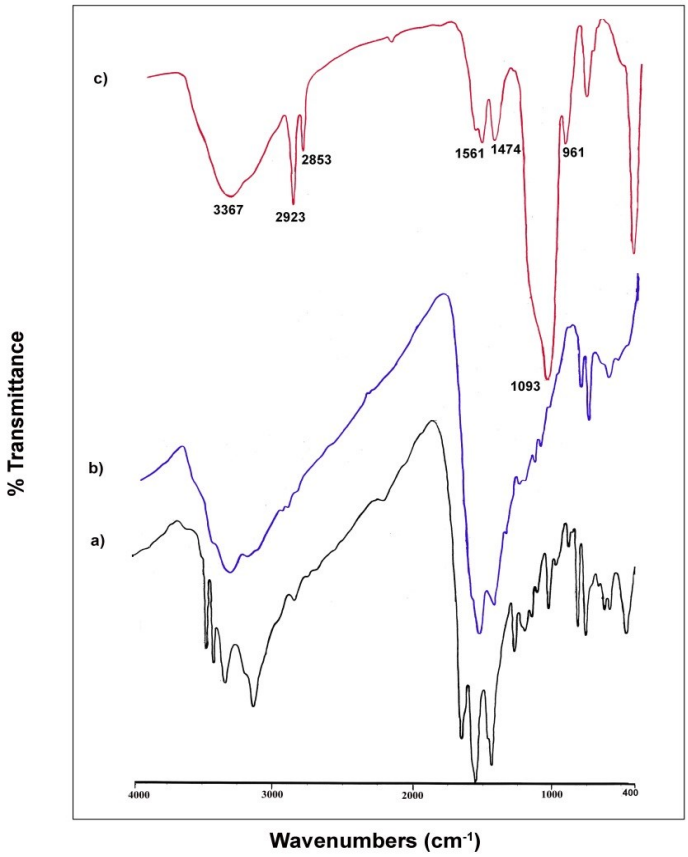

Figure S5. FT-IR spectra of a) Ligand b) Copper-complex and c) Cu@MOS NCs.

3. FT-IR spectra of the Synthesized Compounds

2-Amino-4-(4-chlorophenyl)-7,7-dimethyl-5-oxo-5,6,7,8-tetrahydro-4*H*-chromene-3-carbonitrile (**4a**)

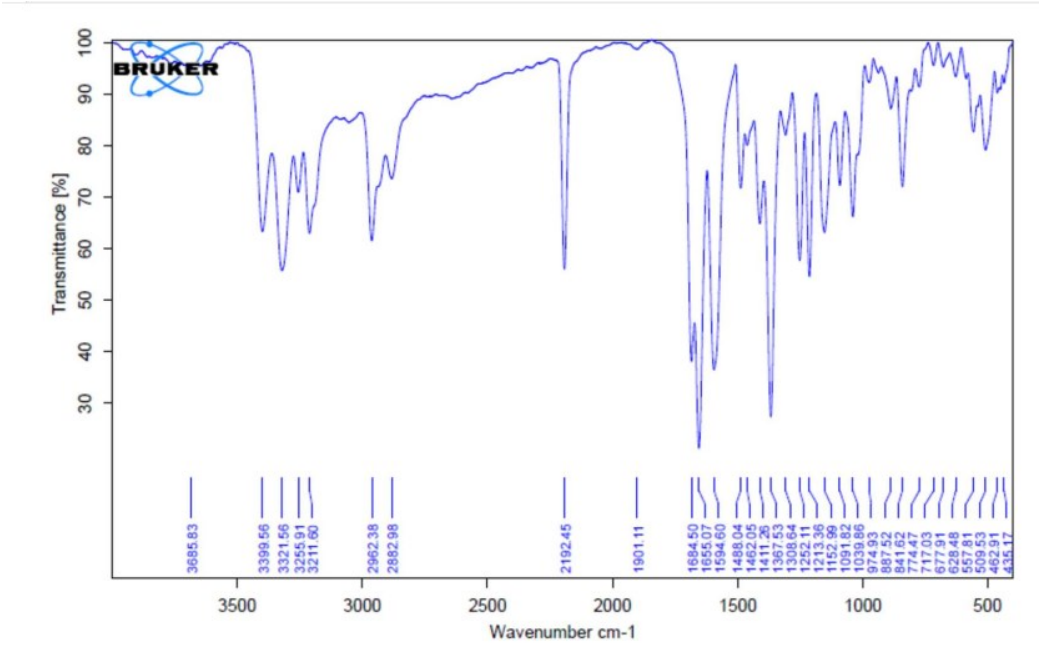

2-Amino-4-(2,4-dichlorophenyl)-7,7-dimethyl-5-oxo-5,6,7,8-tetrahydro-4*H*-chromene-3-carbonitrile (**4b**)

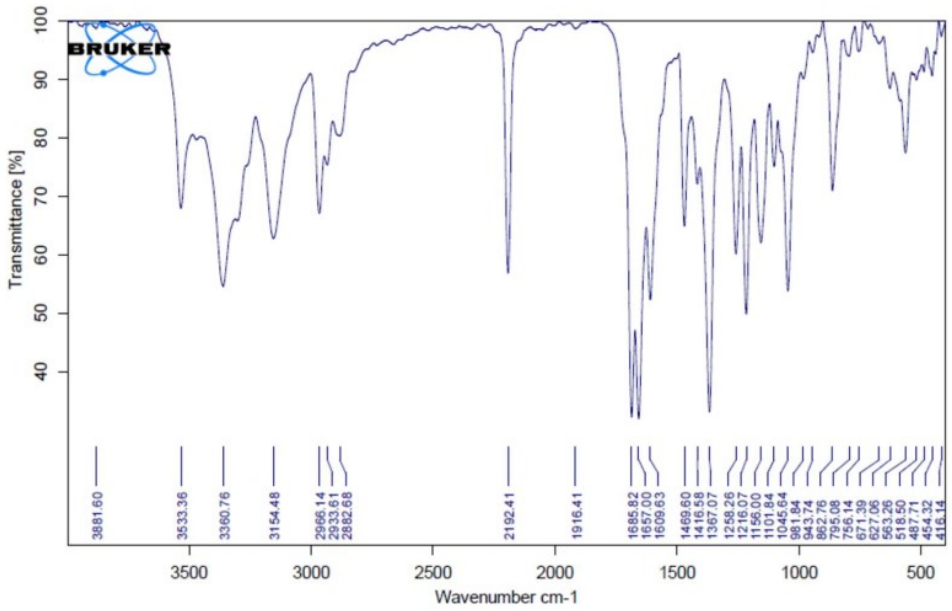

2-Amino-7,7-dimethyl-4-(4-nitrophenyl)-5-oxo-5,6,7,8-tetrahydro-4*H*-chromene-3-carbonitrile (**4c**)

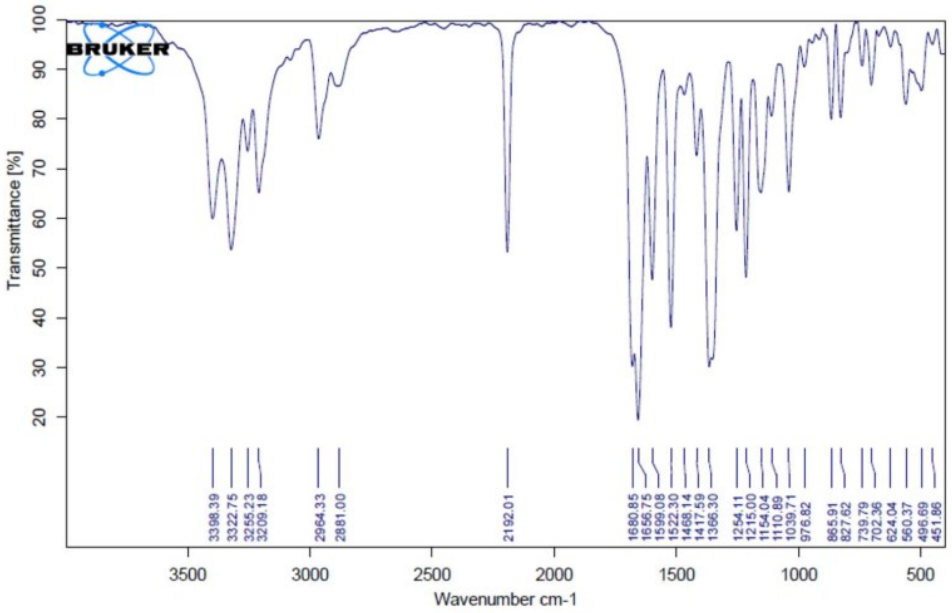

2-Amino-7,7-dimethyl-4-(3-nitrophenyl)-5-oxo-5,6,7,8-tetrahydro-4*H*-chromene-3-carbonitrile (**4d**)

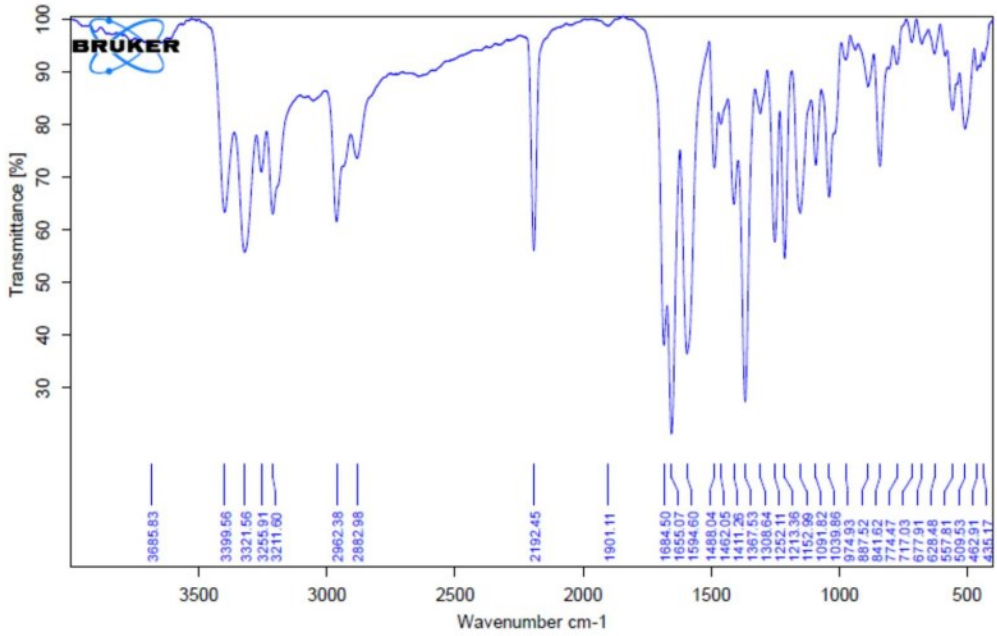

2-Amino-4-(3,4-dimethoxyphenyl)-7,7-dimethyl-5-oxo-5,6,7,8-tetrahydro-4*H*-chromene-3-carbonitrile (**4e**)

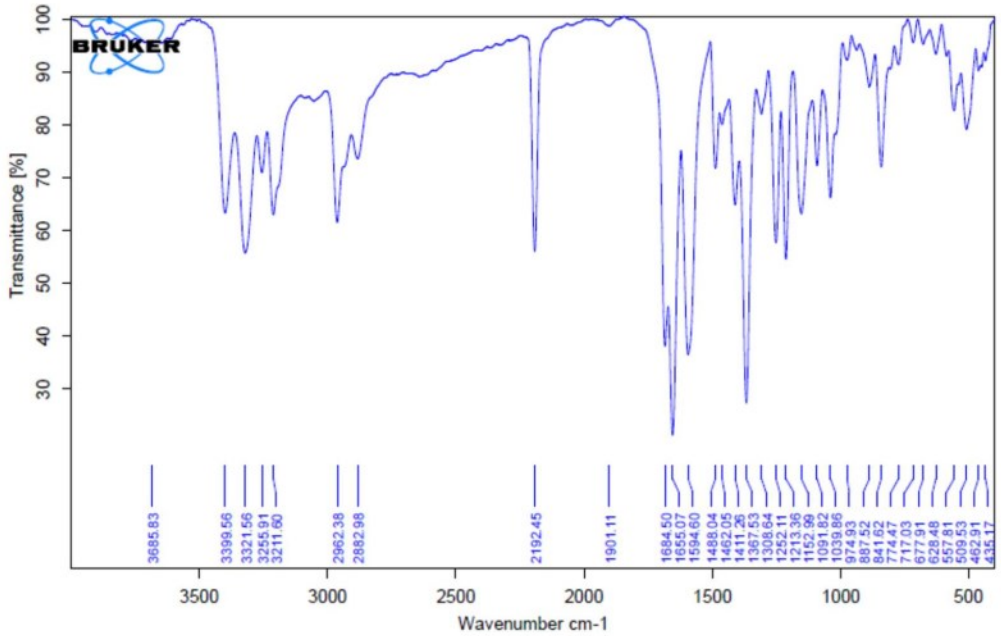

2-Amino-4-(4-hydroxy-3-methoxyphenyl)-7,7-dimethyl-5-oxo-5,6,7,8-tetrahydro-4*H*-chromene-3-carbonitrile (**4f**)

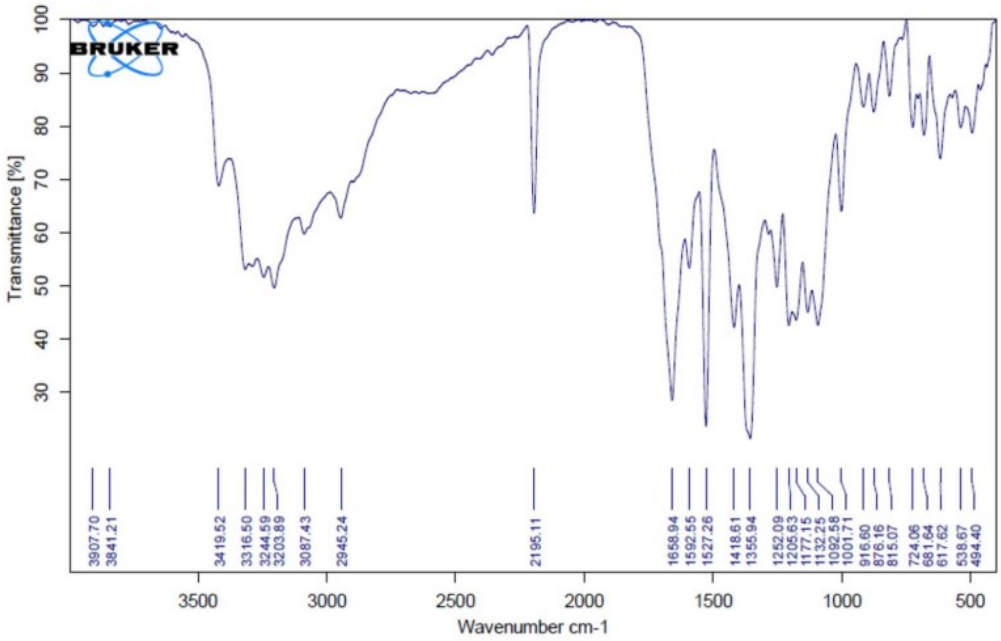

2-Amino-4-(4-chlorophenyl)-5-oxo-5,6,7,8-tetrahydro-4*H*-chromene-3-carbonitrile (**4g**)

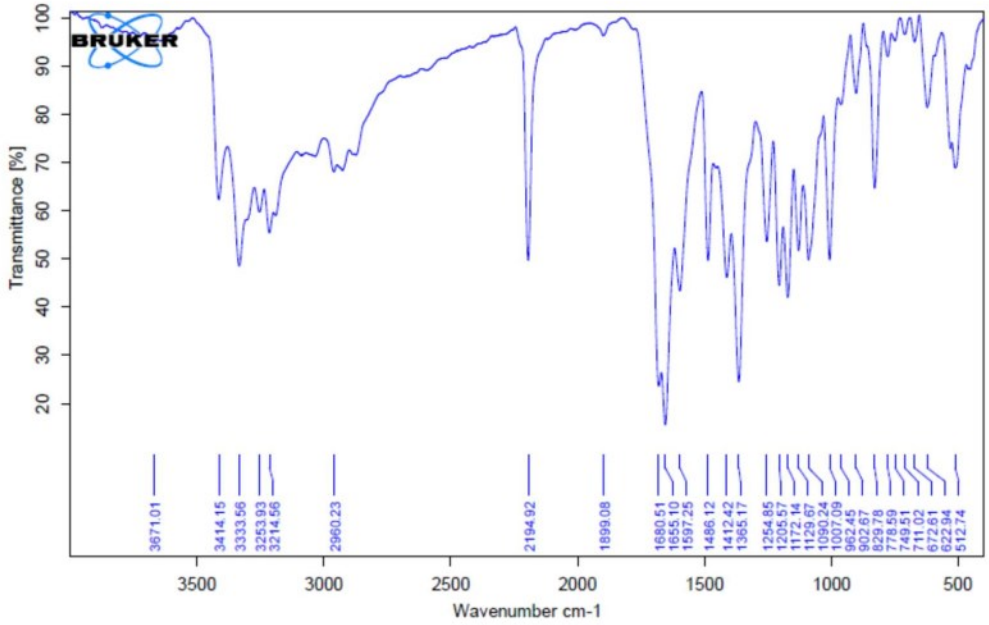

2-Amino-4-(4-nitrophenyl)-5-oxo-5,6,7,8-tetrahydro-4*H*-chromene-3-carbonitrile (**4h**)

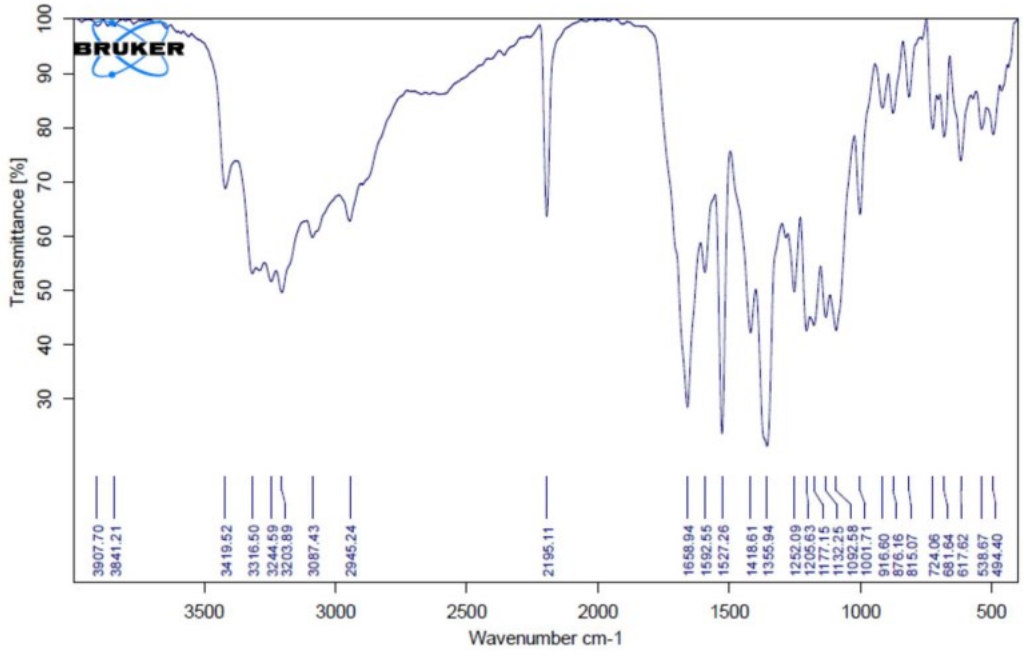

2-Amino-4-(3-nitrophenyl)-5-oxo-5,6,7,8-tetrahydro-4*H*-chromene-3-carbonitrile (**4i**)

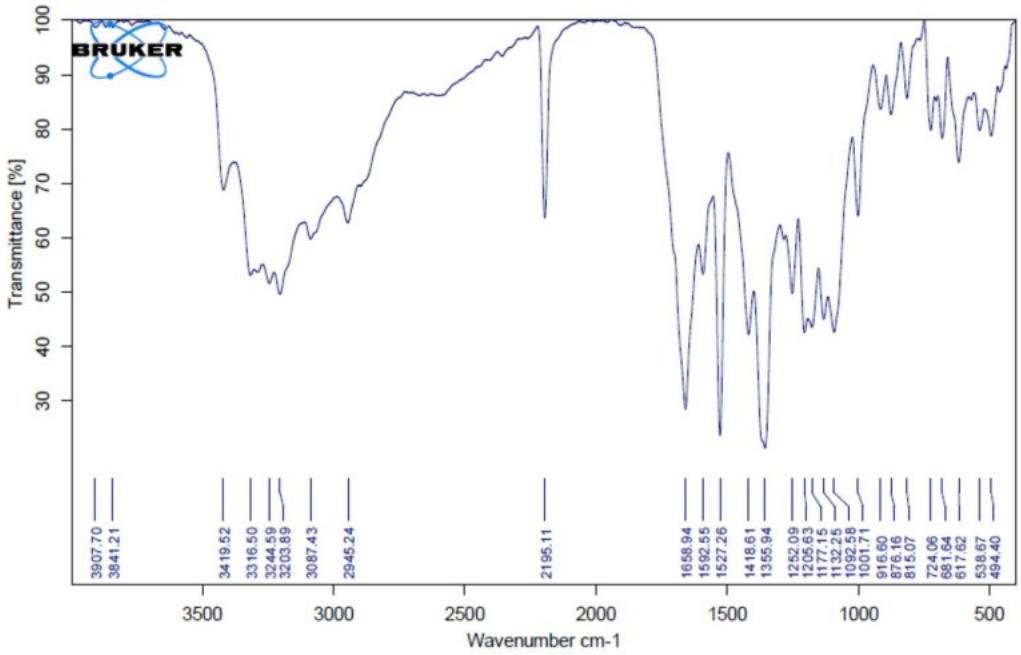

2-Amino-4-(3,4-dimethoxyphenyl)-5-oxo-5,6,7,8-tetrahydro-4*H*-chromene-3-carbonitrile (**4j**)

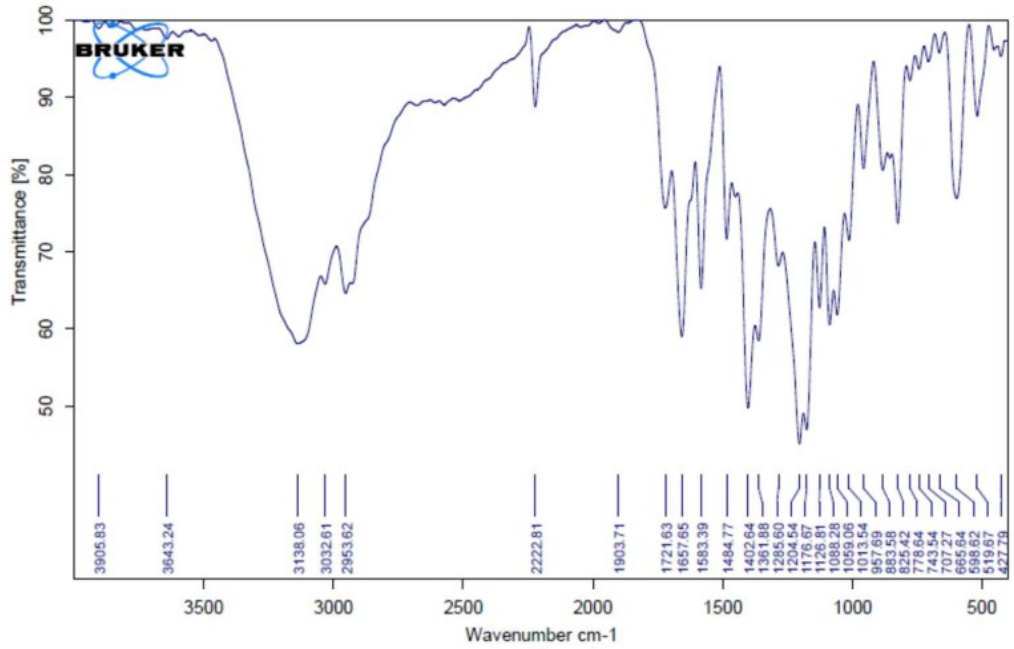

4. ^{1}H NMR Spectra of Some Synthesized Compounds

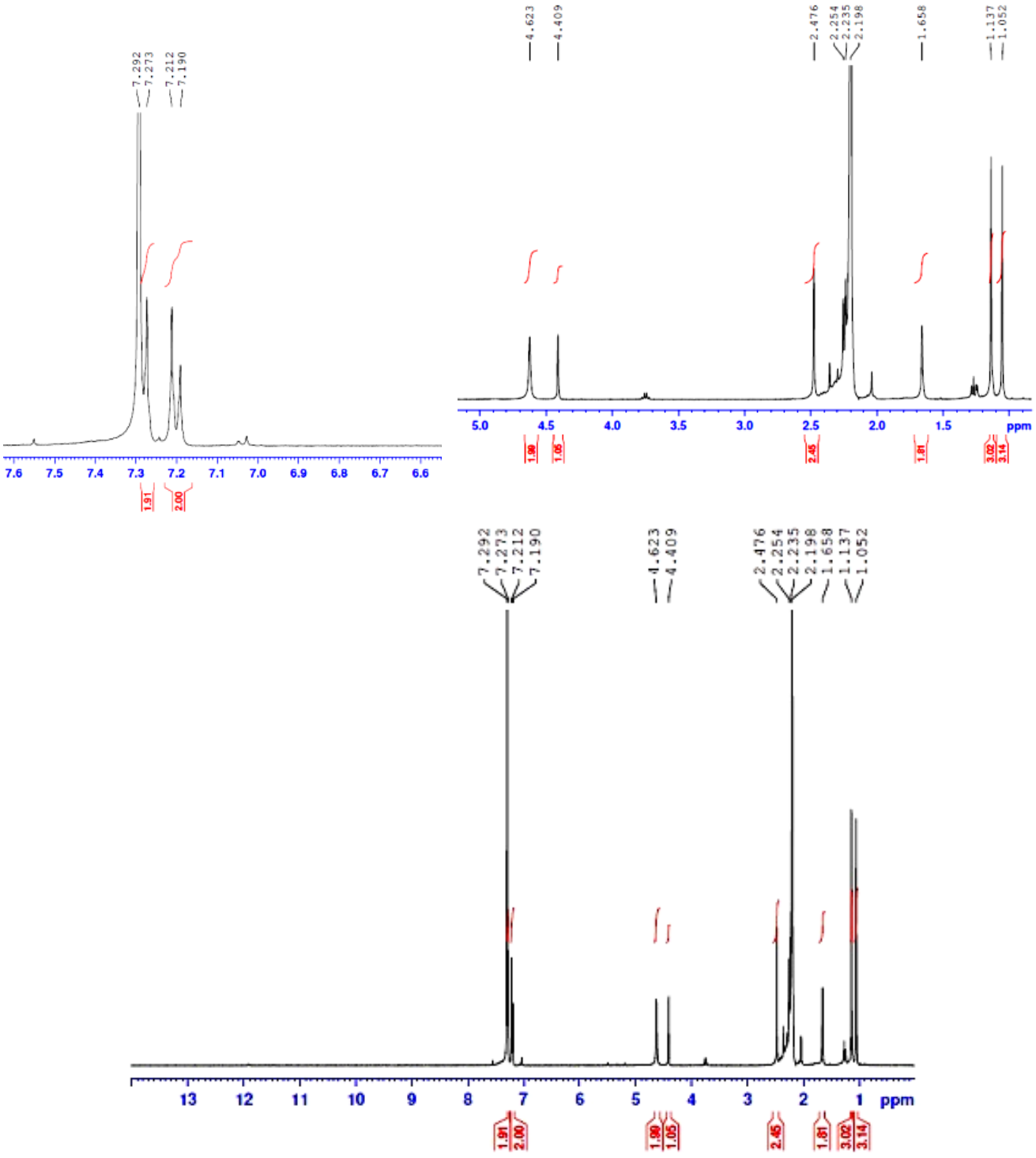

^{1}H NMR spectra for: 2-Amino-4-(4-chlorophenyl)-7,7-dimethyl-5-oxo-5,6,7,8-tetrahydro-4*H*-chromene-3-carbonitrile (**4a**)

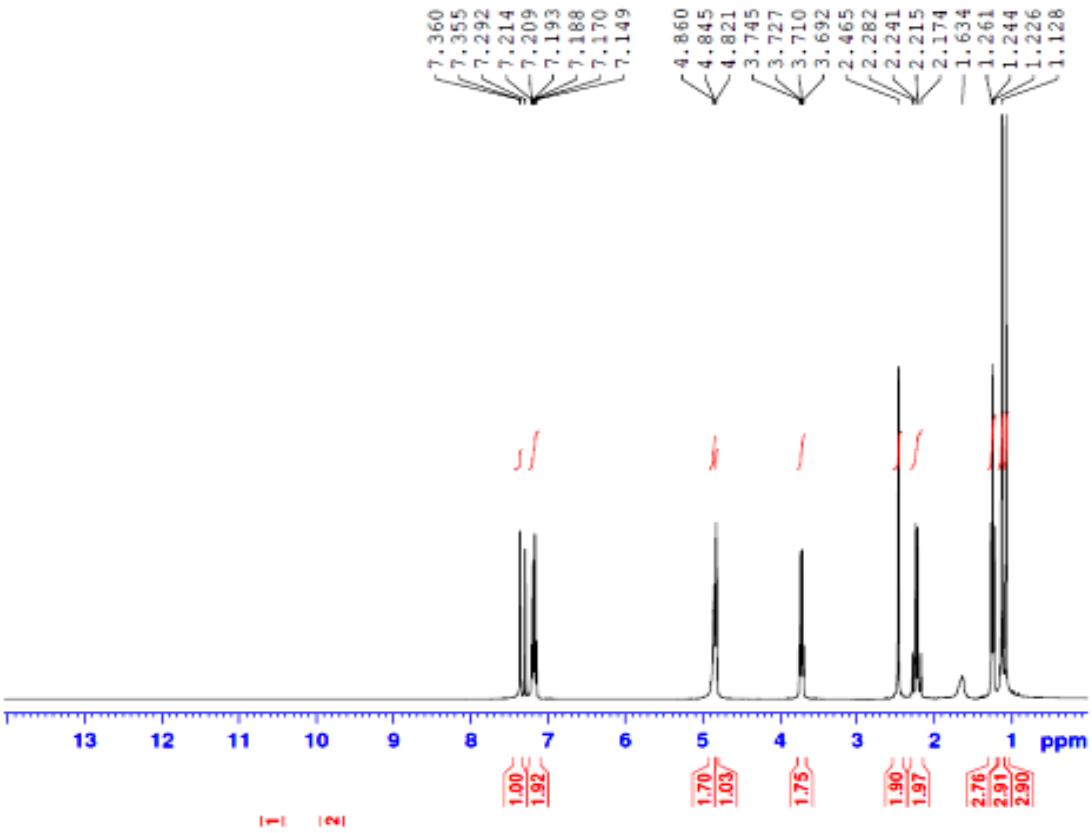

^{1}H NMR spectra for: 2-Amino-4-(2,4-dichlorophenyl)-7,7-dimethyl-5-oxo-5,6,7,8-tetrahydro-4*H*-chromene-3-carbonitrile (**4b**)

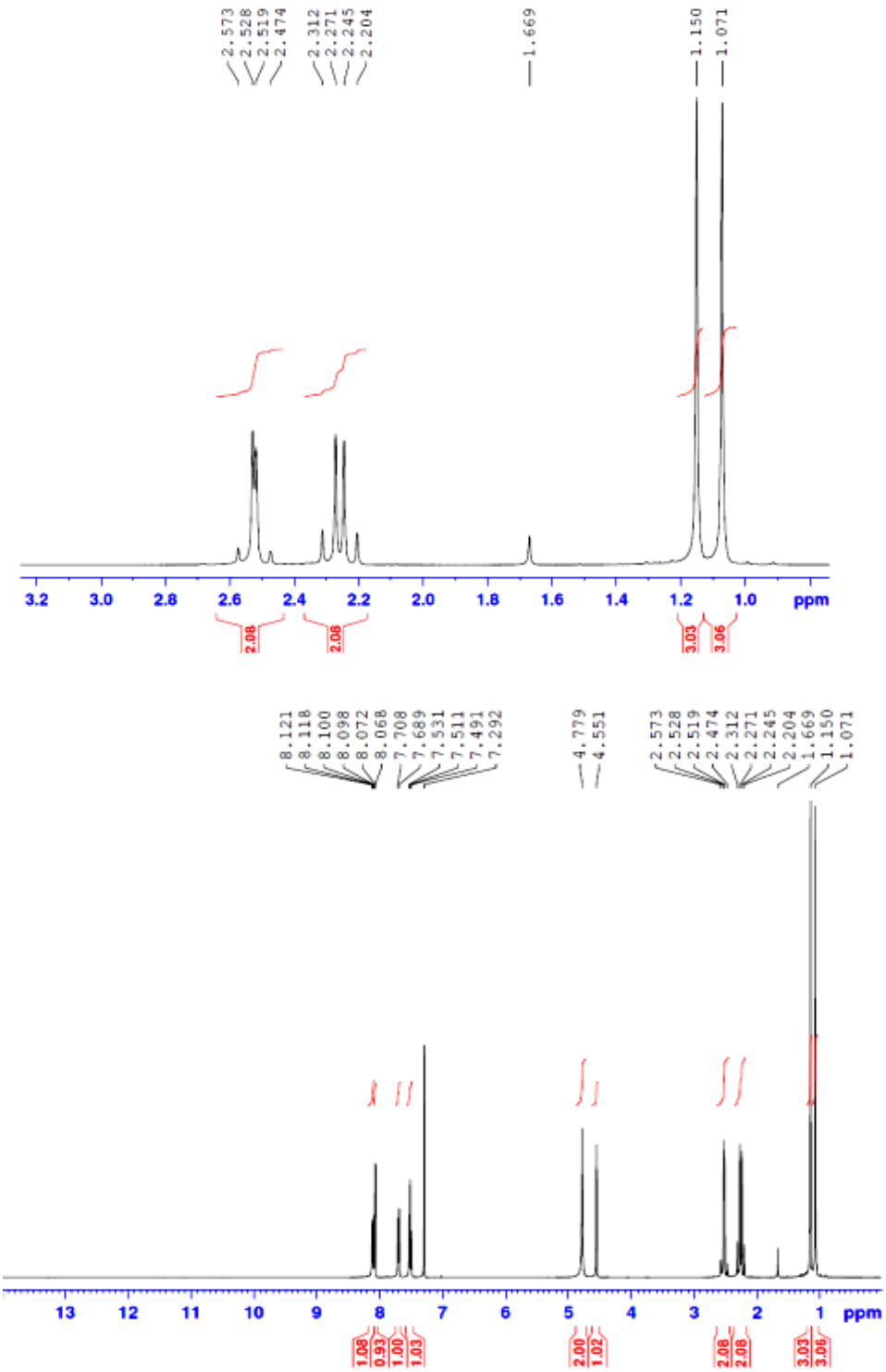

^{1}H NMR spectra for: 2-Amino-7,7-dimethyl-4-(3-nitrophenyl)-5-oxo-5,6,7,8-tetrahydro-4*H*-chromene-3-carbonitrile (**4d**)

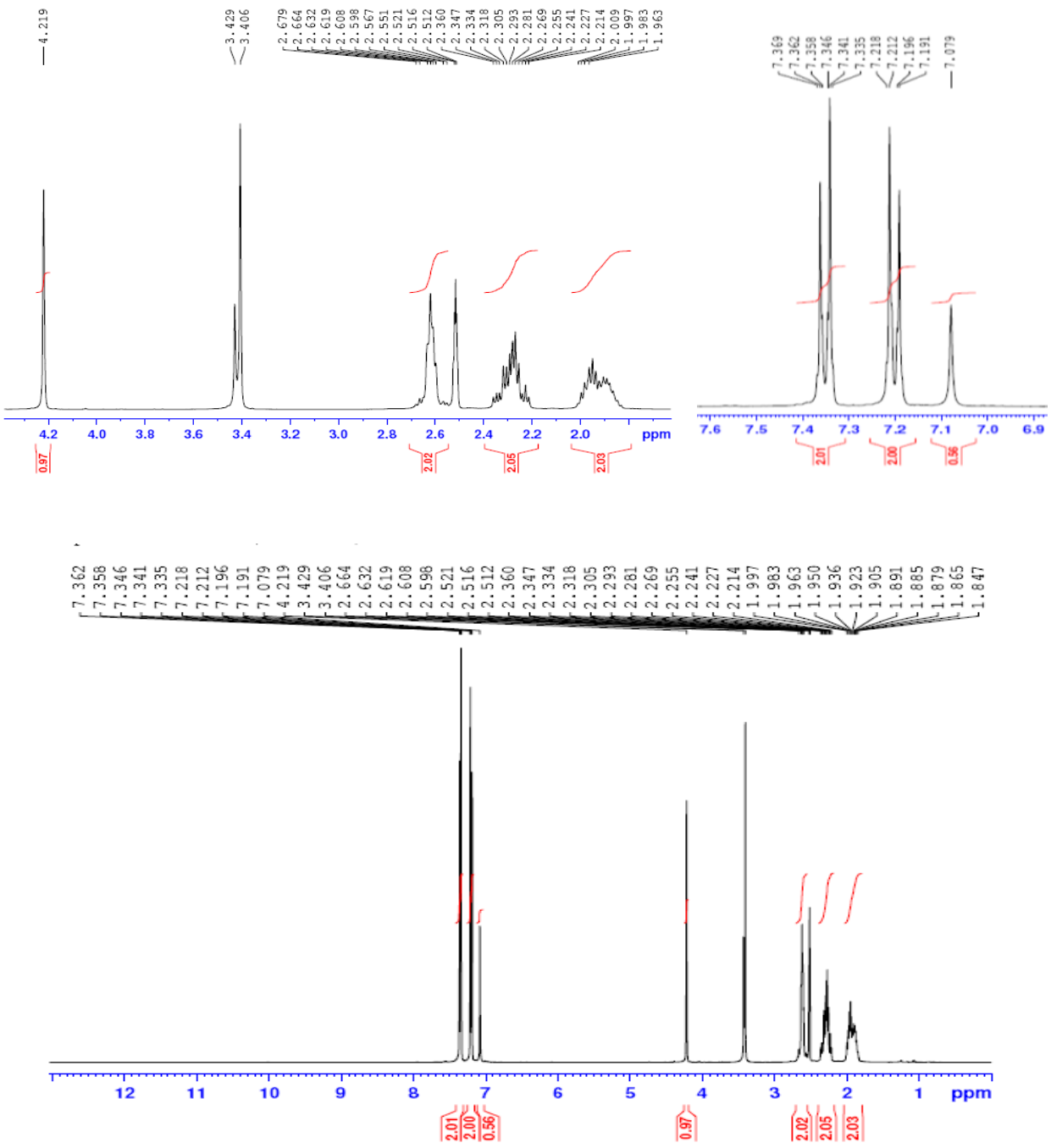

^{1}H NMR spectra for: 2-Amino-4-(4-chlorophenyl)-5-oxo-5,6,7,8-tetrahydro-4*H*-chromene-3-carbonitrile (**4g**)

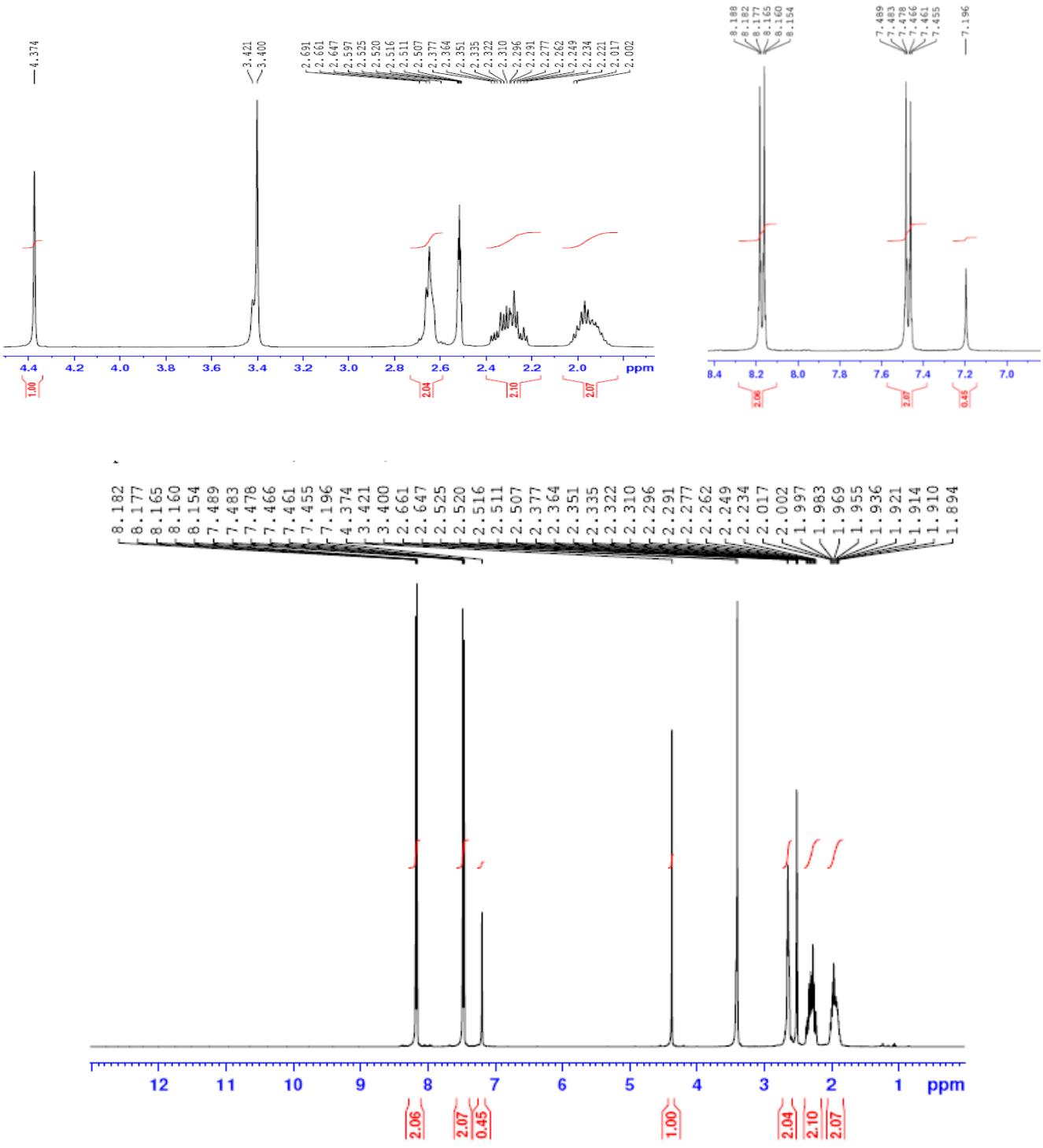

^{1}H NMR spectra for: 2-Amino-4-(4-nitrophenyl)-5-oxo-5,6,7,8-tetrahydro-4*H*-chromene-3-carbonitrile **(4h)**

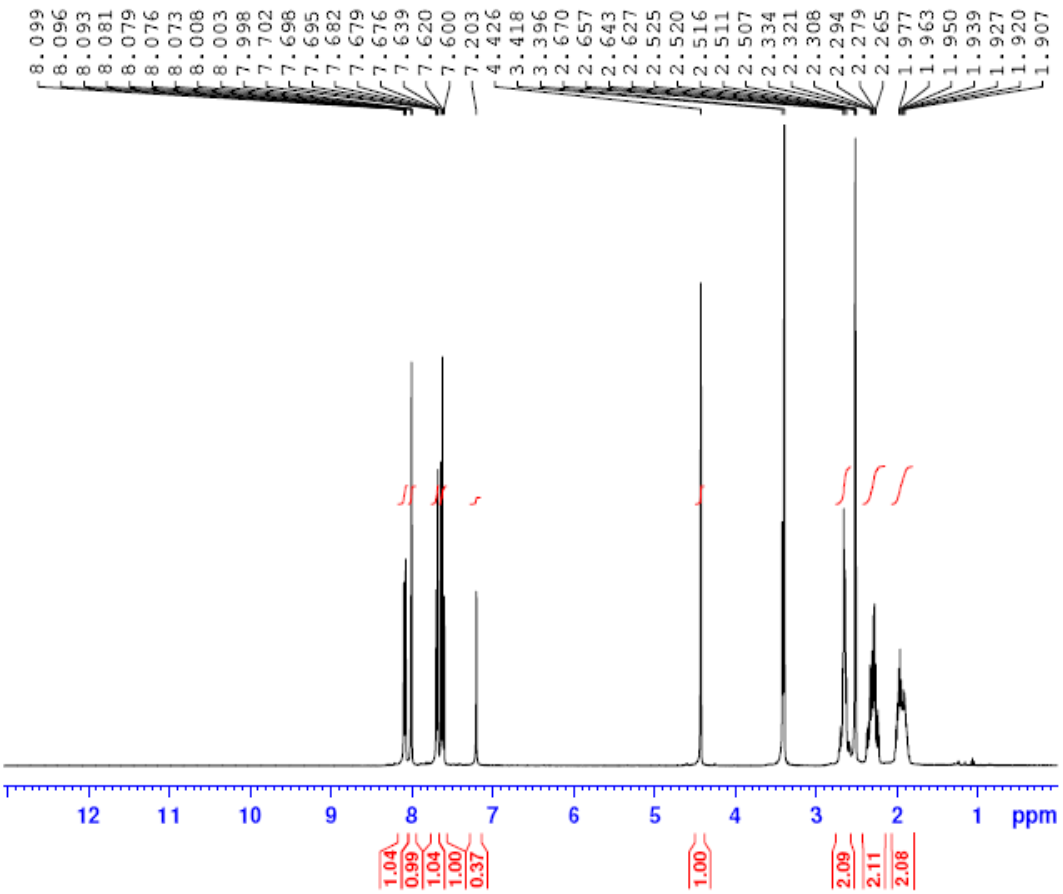

^{1}H NMR spectra for: 2-Amino-4-(3-nitrophenyl)-5-oxo-5,6,7,8-tetrahydro-4*H*-chromene-3-carbonitrile **(4i)**

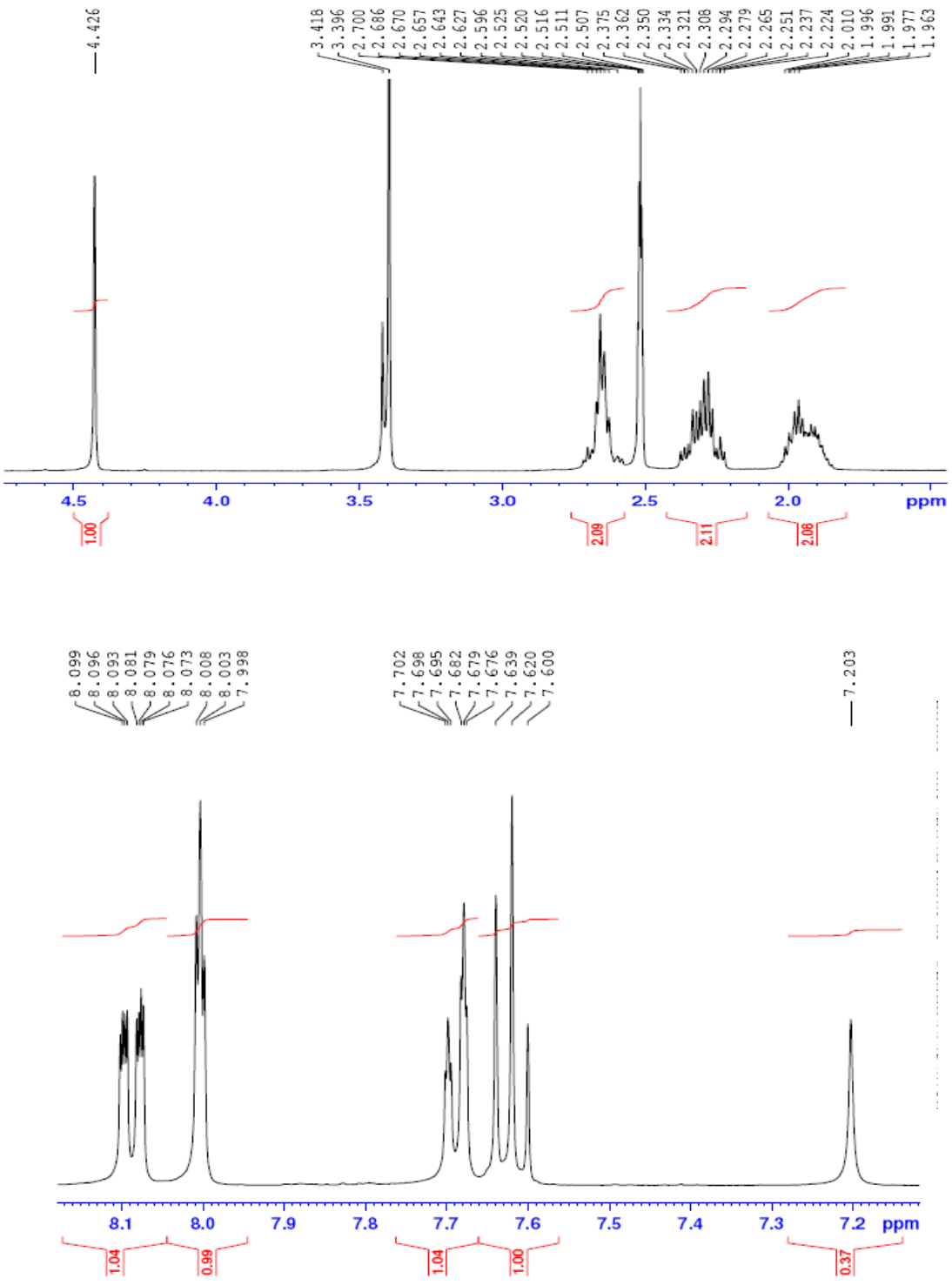

[1]H NMR spectra for: 2-Amino-4-(3-nitrophenyl)-5-oxo-5,6,7,8-tetrahydro-4*H*-chromene-3-carbonitrile **(4i)**